



OPEN Graphene and its modifications for enhanced adhesion in dental restoratives: a molecular docking and dynamics study

Mohammad Ali Saghiri¹, Ravinder S Saini², Mohamed Saheer Kuruniyan³,
Seyed Ali Mosaddad^{4,5,6}✉ & Artak Heboyan⁷✉

Graphene has attracted significant attention in dentistry due to its structural and adhesive properties, enhancing the mechanical performance of dental composites. This study investigates the behavior and interaction of monomers and graphene-based adhesives using molecular docking and molecular dynamics (MD) simulations. Binding energies and interactions between monomers and graphene derivatives were assessed using molecular docking, while MD simulations with the Forcite module and COMPASS II force field provided insights into the mechanical properties of the composites. The simulations involved energy minimization, NVT/NPT ensembles, and equilibration for 50 ns. The binding energies of the monomer-graphene complexes ranged from -16.27 to -18.55 kcal/mol, with the Bis-GMA-Graphene Quantum Dot complex showing the most stable interaction. Mechanical properties such as Young's modulus, shear modulus, and flexural strength were calculated for selected complexes: Bis-GMA-Graphene Quantum Dot (14.74 GPa, 9.32 GPa, 120.51 MPa), EBPADMA-Graphene Quantum Dot (14.28 GPa, 9.13 GPa, 118.22 MPa), HEMA-Nitrogen-doped Graphene (9.85 GPa, 6.86 GPa, 95.7 MPa), TEGDMA-Graphene Oxide (11.96 GPa, 8.12 GPa, 110.23 MPa), and UDMA-CCOOH Functionalized Graphene (13.82 GPa, 8.43 GPa, 115.4 MPa). The Bis-GMA-Graphene Quantum Dot complex showed the highest stability with 20 hydrogen bonds. These results highlight graphene quantum dots and functionalized graphene derivatives as promising candidates for high-performance dental composites, offering strong adhesive properties and improved mechanical strength. Future research may focus on further optimizing these interactions and exploring additional graphene modifications.

Keywords Dental composites, Graphene-based dental adhesives, Mechanical properties, Monomers, Molecular docking, Molecular dynamics simulations

Abbreviations

AIRs	Ambiguous interaction restraints
Bis-GMA	Bisphenol A glycidyl methacrylate
DFT	Density functional theory
EBPADMA	Ethoxylated Bisphenol A dimethacrylate
FDA	Food and Drug Administration
GQDs	Graphene quantum dots
GO	Graphene oxide
HEMA	2-Hydroxyethyl methacrylate

¹Department of Restorative Dentistry, Director of Biomaterial and Prosthodontic Laboratory, Rutgers School of Dental Medicine, Newark, NJ, USA. ²Department of Dental Health Sciences COAMS, King Khalid University, Abha, Saudi Arabia. ³Department of Dental Technology, COAMS, King Khalid University, Abha, Saudi Arabia. ⁴Department of Research Analytics, Saveetha Institute of Medical and Technical Sciences, Saveetha Dental College and Hospitals, Saveetha University, Chennai, India. ⁵Department of Conservative Dentistry and Buccofacial Prosthesis, Faculty of Odontology, Complutense University of Madrid, Madrid, Spain. ⁶Department of Prosthodontics, School of Dentistry, Shiraz University of Medical Sciences, Qasr-e-Dasht Street, Shiraz, Fars, Iran. ⁷Department of Prosthodontics, Faculty of Stomatology, Yerevan State Medical University after Mkhitar Heratsi, Str. Koryun 2, Yerevan 0025, Armenia. ✉email: Mosaddad.sa@gmail.com; heboyan.artak@gmail.com

MD	Molecular dynamics
NPT	Number of particles, system pressure, and temperature
NVT	Number of particles, system volume, and temperature
PME	Particle mesh Ewald
PRODIGY	PROtein binDing enerGY prediction
rGO	Reduced graphene oxide
RMSD	Root means square deviation
SDF	Structure data format
TEGDMA	Triethylene glycol dimethacrylate
UDMA	Urethane dimethacrylate

Dental restorative materials restore decayed or damaged teeth and thus maintain dental health, function, and appearance. The durability of such restorations depends upon the adhesive systems that adhere the restoration material to the tooth's structure¹. Effective adhesion is necessary to ensure the longevity and durability of the restorations, minimize microleakage, and decrease secondary caries and restoration failure^{2,3}. The matrix of dental resin composites is usually a 3D network made up of bisphenol-a-glycidyl methacrylate (Bis-GMA) mixed with triethylene glycol dimethacrylate (TEGDMA) monomers⁴. These substances also come with many advantages, like the comfort of handling and appearance. However, even dental resin composites are not without their limitations: poor bonding with tooth surfaces and a poorly adapted biomechanical function relative to ceramics or amalgam^{5,6}. Adhesion is very important to ensure the longevity of tooth restorations⁷. Microleaking at the composite/tooth contact can result in secondary caries and restoration failure. Also, dental composites are typically weaker in flexural strength and fracture toughness than natural materials and, therefore, less able to withstand the severe forces that chewing puts on teeth^{8,9}. The bond between tooth structure and dental fillings must resist physical and chemical forces in the mouth. Some of the commonly faced issues are the formation of a durable connection, shrinkage of polymerization, biocompatibility, and antimicrobial properties to keep the bacterial community from colonizing and forming biofilms^{10,11}. Current adhesive systems, although effective up to a point, are inadequate in these respects, which results in loss of restoration and repeated replacement.

Graphene is a two-dimensional carbon allotrope composed of a single layer of atoms, structured in a hexagonal lattice, and has received attention across different areas due to its incredible mechanical, electrical, and thermal performance^{12,13}. Its high surface area, mechanical strength, and functional properties render it a potential candidate for the enhancement of dental composites^{14,15}. Graphene, when incorporated into dental adhesives, could resolve some of these issues by enhancing the mechanical properties and biocompatibility of the adhesives^{16,17}. We can also chemically synthesize the graphene in additional ways to improve its properties and performance against dental enamel. Typical transformations are the oxidation of graphene-to-graphene oxide (GO), reduction of GO to reduce graphene oxide (rGO), and functionalization with polymers and molecules^{18,19}. These changes can optimize the hydrophilicity, reactivity, and mechanical properties of graphene for certain applications. GO's hydrophilicity, for instance, optimizes the dispersibility in water, which optimizes the incorporation into dental adhesives^{20,21}. In addition, graphene-based nanomaterials have also been tested as a means to enhance the performance of dental adhesives with greater adhesion and shrinkage from polymerization^{22,23}. Dental restoratives are bonded to a tooth substrate through chemical and physical interaction between the monomers of the adhesive and the tooth material. These factors – including the type of adhesive monomers, functional groups, and the mechanical stability of the adhesive layer – play an important role in making a bond strong and durable^{24,25}. It is important to know about these molecular interactions to produce adhesives that will form solid, stable connections to the tooth structure and that will withstand degradation over time. These problems can be better addressed with dental adhesives that are able to take advantage of the special attributes of graphene and its modification. In recent studies, the potential of graphene-based nanomaterials to enhance the interfacial properties and mechanical strength of nanocomposites has been explored. One study investigated the effect of grain boundaries on the interfacial properties of bi-crystalline graphene/polyethylene-based nanocomposites using molecular dynamics simulations²⁶. The findings revealed that the higher energy states at the grain boundaries of bi-crystalline graphene improved interactions at the nanocomposite interphase, and the geometrical imperfections, such as wrinkles and ripples, enhanced adhesion between the nanofiller and matrix. Another study reviewed the use of graphene and hexagonal boron nitride (h-BN) nanofillers in polymer-based nanocomposites, highlighting their exceptional mechanical, thermal, and electrical properties²⁷. The study discussed the potential of atomistic modeling techniques to predict the mechanical properties and fracture toughness of these nanocomposites, underlining the importance of accurate interatomic potentials for successful simulations.

In this study, molecular docking and molecular dynamics (MD) simulations were employed to investigate the interactions between a single dental adhesive monomer and a small graphene flake in both its pristine and functionalized states. The goal was not to model a complete polymeric dental composite but rather to provide fundamental molecular insights into monomer–graphene interactions as a preliminary step toward designing improved graphene-based dental adhesives. Molecular docking was used to predict the binding conditions and specificity of the monomer on different graphene surfaces, identifying key interaction sites and favorable adhesion mechanisms. Following docking, MD simulations were performed to examine the stability and dynamic behavior of these monomer–graphene complexes over time. MD simulations have become a valuable tool in dental materials research, as they enable atomic-scale insights into interaction mechanisms that influence adhesion and mechanical behavior²⁸. The primary motivation for this study stemmed from the growing interest in using graphene and its derivatives to enhance the adhesive and mechanical properties of dental composites. Despite the recognized potential of graphene-based materials, there remains a gap in understanding how monomers interact at the molecular level with different graphene surfaces. Specifically, this study addresses

the fundamental question of how different functionalized graphene surfaces influence monomer adhesion and stability, rather than attempting to model a fully polymerized system. To further strengthen our computational approach, stress-strain calculations were performed to evaluate the mechanical response of the monomer-graphene complexes. We have now explicitly described how the system was built, including atomistic details of the simulated structures and the directions along which stress and strain were applied. This approach allowed us to extract fundamental insights into the nanoscale biomechanical behavior of monomer-graphene interactions, which can serve as a foundation for future research incorporating polymeric chains and larger-scale composites. The novelty of this work lies in its systematic computational exploration of monomer-graphene interactions using molecular docking and MD simulations. By identifying key adhesion trends and mechanical properties, this study provides valuable insights that can be leveraged in the development of high-performance dental composites. Furthermore, our findings highlight promising graphene derivatives, such as graphene quantum dots and functionalized graphene, as potential candidates for optimizing dental adhesive formulations.

Methodology

Here, the strategy was a methodological, encompassing effort to evaluate and enhance the adhesion and biomechanical attributes (Young's modulus, shear modulus, flexural strength) of dental monomers as well as graphene and its derivatives. This was done with molecular docking and dynamic simulations. The following section outlines the required steps and their relevance to research objectives.

Selection of dental monomers for study

This involved picking individual dental monomers based on composition and performance as reported by published market data. This was based on independent judgment and selection of monomers suitable for the study. These range from chemistry to graphene compatibility to dental adhesive properties (Table 1). Similarly, such monomers must also be exploited to identify the relationship between graphene and dental adhesives. Figure 1 presents the Monomers used in the analysis.

The reason was the need to represent a wide range of materials used in practice. It was a step that matched other studies showing that material composition was a critical influence on the mechanical and adhesive performance of dental resin²⁹. And by pursuing such a diverse range of substrates, the work might find applications in everyday clinical settings. With this interdisciplinary approach, the results of the study would be applicable to clinical cases of a wide variety and provide useful knowledge for dentists and researchers.

Graphene-based dental adhesives selection

The graphene-based dental adhesives were chosen for this paper as we wanted to experiment with various graphene changes and their effect on the dental adhesive (Table 2). Graphene with superior mechanical, thermal, and electrical properties has been used to develop better dental materials^{23,30}. Graphene treatments like chemical doping and functionalization were believed to make it more useful and compatible in dentistry. The functionalized graphene samples in our study are represented by their chemical formulas: $C_{60}H_{37}S_7$ (sulfur-functionalized graphene), $C_{60}H_{44}F_7$ (fluorine-functionalized graphene), and $C_{60}H_{25}N_7$ (nitrogen-functionalized graphene). The weight percentages of sulfur (S), fluorine (F), and nitrogen (N) were calculated based on the

Component	Chemical Structure	Density (g/cm ³)
Monomers		
Bisphenol A glycidyl methacrylate (Bis-GMA)		1.16
Ethoxylated Bisphenol A dimethacrylate (EBPADMA)		1.12
2-Hydroxyethyl methacrylate (HEMA)		1.03
Triethylene glycol dimethacrylate (TEGDMA)		1.07
Urethane dimethacrylate (UDMA)		1.11

Table 1. Chemical structure and density of selected dental monomers.

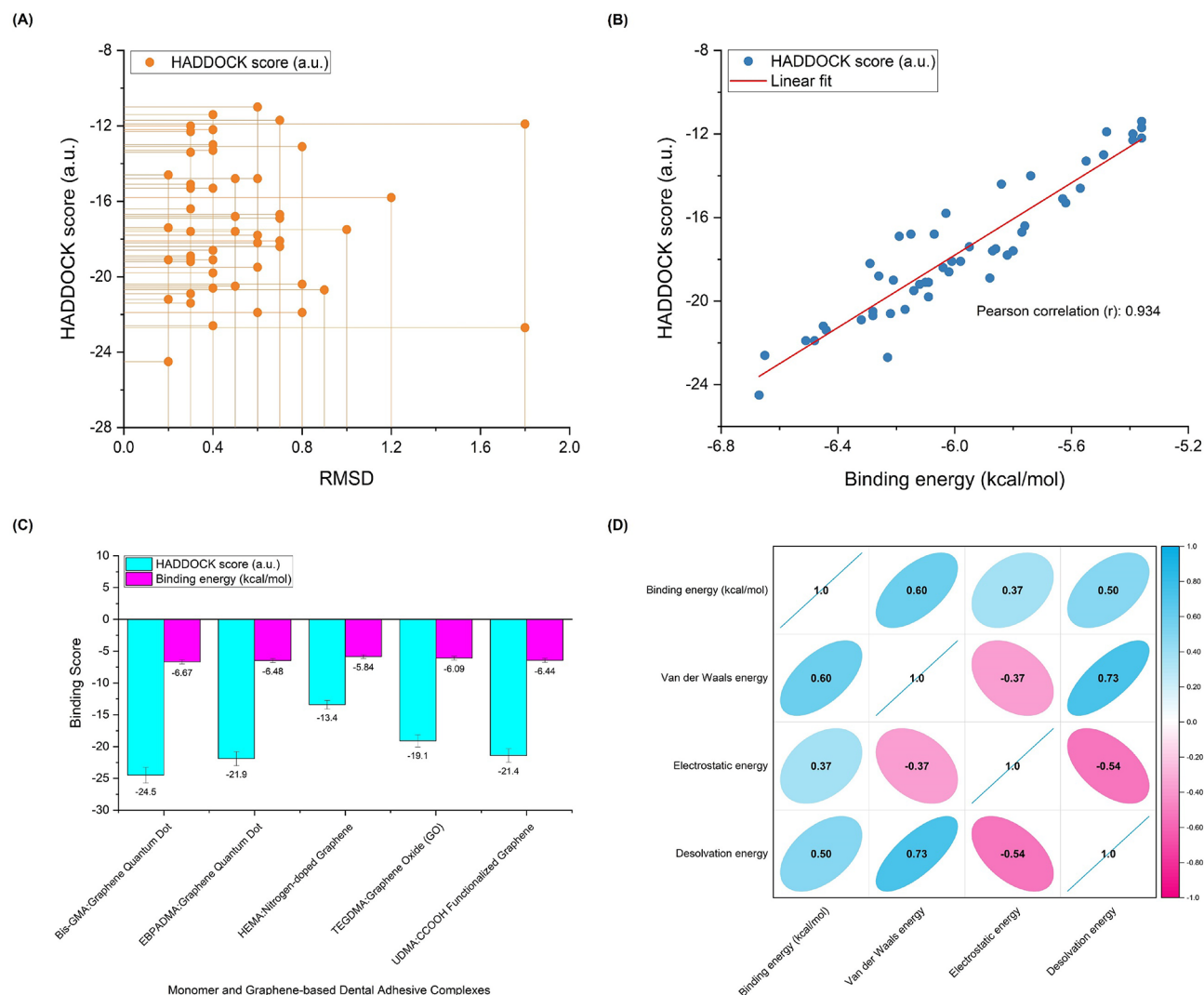
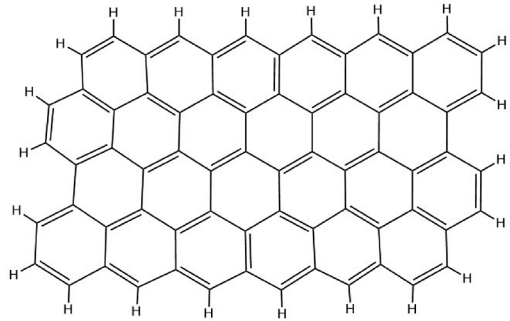
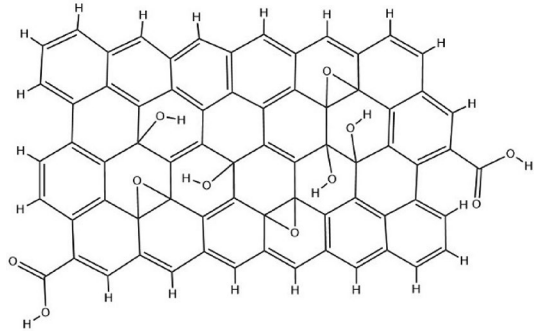
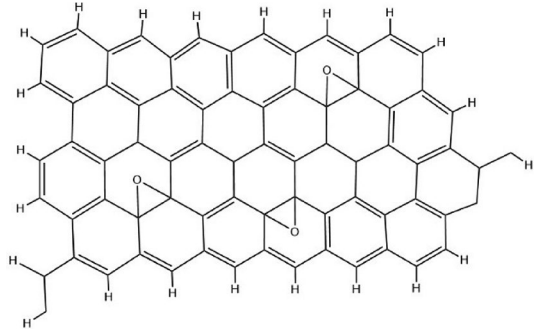
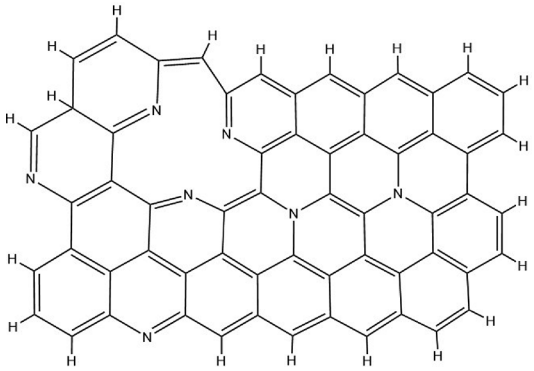
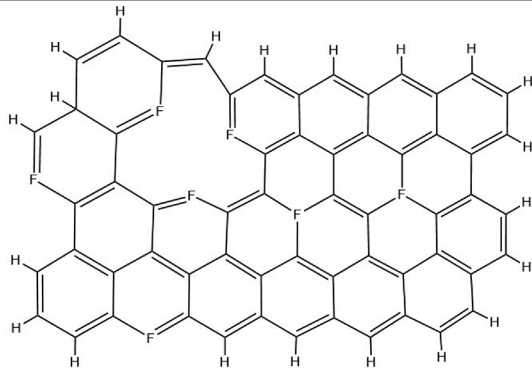
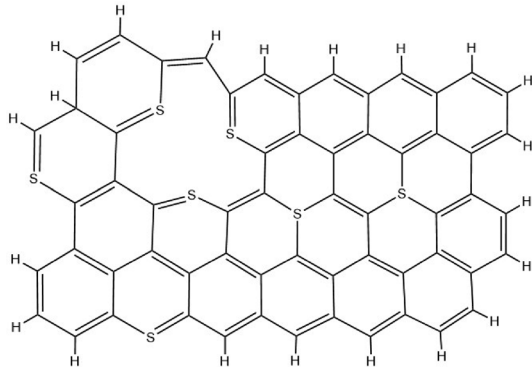
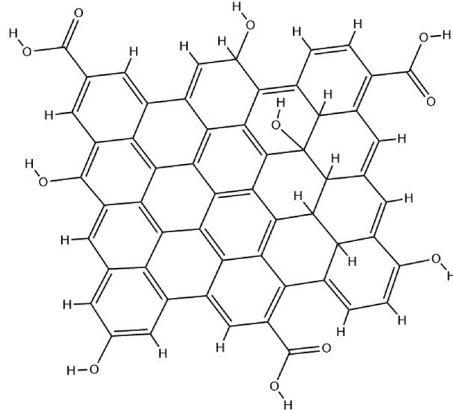
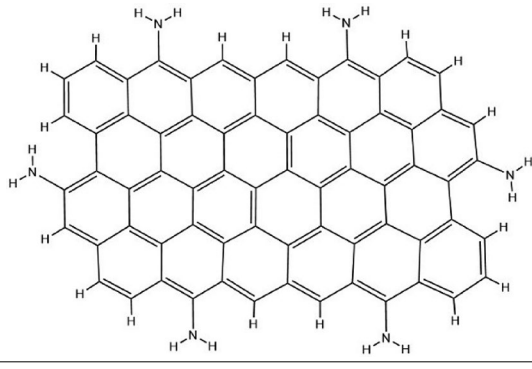


Fig. 1. Molecular docking results overview. **(A)** Relationship between HADDOCK score and Root Mean Square Deviation (RMSD). **(B)** Correlation between HADDOCK score and binding affinity, showing a strong Pearson correlation coefficient ($r = 0.934$). **(C)** Optimal monomer-graphene combinations for each monomer type, highlighting the lowest binding energy values indicative of superior adhesion strength. **(D)** Correlation matrix depicting the relationship between binding energy (kcal/mol) and individual energy components.

molecular weights of the functionalized groups and the graphene backbone. The rationale for selecting these particular functionalization patterns was driven by the well-established ability of these elements to enhance the interaction between graphene and dental monomers, improving the adhesion and mechanical properties of the resulting composites. In terms of how increasing or decreasing the proportion of these functional groups might affect the results, increasing the sulfur content (as in $C_{60}H_{37}S_7$) could enhance the dispersibility and flexibility of the functionalized graphene in the resin matrix but might reduce material strength if the sulfur content becomes excessive. Fluorine ($C_{60}H_{44}F_7$) is known to increase surface polarity and promote stronger interactions with hydrophobic monomers, improving strength and stability, although too much fluorine could disturb the balance between adhesion and mechanical strength. Lastly, nitrogen ($C_{60}H_{25}N_7$) can strengthen the interaction with amine groups in the monomers, improving adhesion. However, excessive nitrogen could compromise the composite's overall stability and rigidity.

High-purity graphene was chosen as the initial material due to its basic characteristics, tensile strength, electrical conductivity, and vast surface area³¹. These properties are crucial to exploring the major dental adhesive advantages of graphene: mechanical toughness and superior bonding with dental monomers. GO was chosen due to its hydrophilic properties and a high quantity of oxygen-rich functional groups, which could help it disperse in water and interact more effectively with dental adhesive monomers³². GO's hydrogen bonding capabilities with other materials make it an ideal candidate for improving the bonding capability of dental restorations. Reduced graphene oxide provides a compromise between pristine graphene and graphene oxide. It retains some oxygen functional groups but re-establishes most of graphene's electrical conductivity³³. Nitrogen-doped, fluorine-doped, and sulfur-doped graphene were used as they could impart active sites for

Component	Chemical Structure	Molecular weight (g/mol)
Graphene-based dental adhesive		
High-Purity Graphene		838.9
Graphene Oxide (GO)		1042.9
Reduced Graphene Oxide (rGO)		946.9
Nitrogen-doped Graphene		839.9
Continued		

Component	Chemical Structure	Molecular weight (g/mol)
Graphene-based dental adhesive		
Fluorine-doped Graphene		817.5
Sulfur-doped Graphene		966.3
Graphene Quantum Dot		886.8
NH ₂ Functionalized Graphene		929.0
Continued		

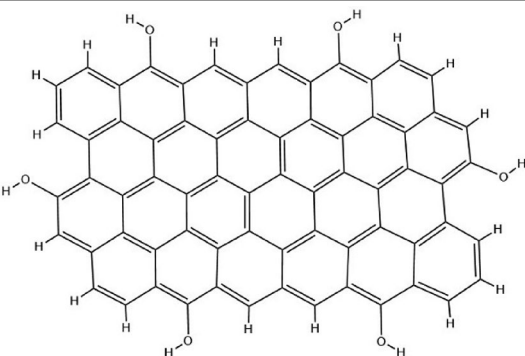
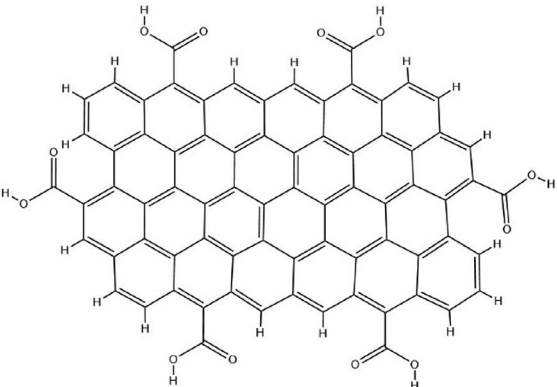
Component	Chemical Structure	Molecular weight (g/mol)
Graphene-based dental adhesive		
COH Functionalized Graphene		934.9
CCOOH Functionalized Graphene		1103.0

Table 2. Chemical structure and molecular weight of high-purity graphene and its modifications.

increased chemical responsiveness and adhesion with dental monomers. Furthermore, these doped graphenes have special attributes of higher chemical resistance and modified electronic properties, which can improve the functionality of dental adhesives^{34,35}. Graphene quantum dots (GQDs) were added because they are nanosized and incredibly unique in terms of their optical capabilities. Thanks to the large surface-to-volume ratio, GQDs can improve mechanical properties and yield additional functionalization locations^{36,37}. NH₂ functionalized graphene was selected because it possesses high covalent bonds to dental adhesive monomers with the aid of amine groups³⁸. These graphenes were functionalized with COH and CCOOH hydroxyl groups selected for improved hydrophilicity and contact with the adhesive monomers. Hydroxyl groups can produce hydrogen bonding and better dispersion in the adhesive matrix³⁹.

3D molecular modeling of monomers and graphene-based dental adhesives

In this section, we discuss the key steps involved in creating 3D models of the complex molecules for monomers and graphene-based dental adhesives. These computational models provide the foundation on which we can interpret the molecular forces that control the behavior and performance of these composites. These steps were carefully followed to be exact and robust in our modeling approach. It was necessary to get good 3D representations of all the components (monomers, graphene dental adhesives). Ligands corresponding to these molecules were obtained from the huge PubChem database, a collection of chemical structures. Each ligand was chosen to incorporate several different molecular structures and functions for dental adhesives. Once the molecular structures were bought, a very important minimization step was performed in OpenBabel version 3.0.1⁴⁰. For this geometry optimization process, the MM2 force field⁴¹ was used to minimize the energy and stabilize the structure of each monomer and graphene-based dental adhesive. This process was crucial to maximize the geometry of atoms within a given molecule such that structures were energetically stable and followed the most appropriate spatial distributions. Through minimizing energy, we wanted to get molecular conformations that were representative of the physical structure of dental adhesive elements.

- a. **Monomers:** The molecular structures of some monomers — among them, the most used, 2-Hydroxyethyl methacrylate (HEMA), Bisphenol A glycidyl methacrylate (Bis-GMA), Ethoxylated Bisphenol A dimethacrylate (EBPADMA), triethylene glycol dimethacrylate (TEGDMA) and Urethane dimethacrylate (UDMA) — were precisely determined. It entailed precisely calculating the lengths, angles, and dihedral angles of the bonding bonds to reproduce the three-dimensional shape of each monomer molecule accurately. Such monomers form the building blocks of dental resin matrixes and so contribute to the mechanical strength of the composite.

- b. **Graphene-based dental adhesives:** Ten graphene dental adhesives of varying compositions were selected because they might significantly alter the mechanical behavior of composites. The 3D structures of these graphene-based adhesives were carefully designed in ChemDraw Ultra 12.0 (PerkinElmer Inc.)⁴². This software enabled the spatial and chemical patterns of graphene-based adhesives to be mapped on a level of detail comparable to their real-world equivalent.

These precise steps in 3D molecular modeling constituted a solid foundation for the study of the more nuanced interactions between monomers and graphene-based dental adhesives. This integrated technique allowed structural complexity and elastomer performance to be studied at the molecular level, providing valuable data to design and optimize dental adhesive formulations.

Molecular docking simulations

In this step, we conducted molecular docking experiments using the free HADDOCK, which is a powerful and widely used binding mode and energy exploration software⁴³. Using powerful algorithms, HADDOCK provided a powerful tool for predicting and deciphering the interactions between dental resin composites (monomers and graphene-based dental adhesives). These simulations primarily attempted to predict and understand the interplay between the composite components. Such receptor-less simulations sought to investigate interactions between molecules open-ended and integrated to capture a broad picture of composite behavior. Active parts for each ligand were well-positioned to identify key interaction points, and passive parts for other contributors were also spatially separated to facilitate docking. The addition of AIRs (Ambiguous Interaction Restraints) led to improved predictions, particularly when experimental observations pointed toward approximate binding sites.

2.0 distance constraints established some geometric correspondences between atoms or portions of the two ligands according to structural constraints and facts. Adaptive docking also enabled the ligands to conform in simulation, as do the simulation molecular interactions. After the docking simulations, the resulting docking solutions were clustered to identify representative and stable complexes. This made it possible to find optimal binding patterns, providing insight into the energetically optimal interactions of the composite system. PRODIGY (PROtein binDing enerGY prediction) was also employed to model binding affinity for the monomers and graphene dental adhesive complexes⁴⁴. PRODIGY uses innovative computational methods to calculate the binding potential between molecules and, therefore, find promising candidate complexes for further analysis and experimental confirmation. Combining HADDOCK with PRODIGY, this project explored and assessed the molecular mechanisms of dental adhesive systems to develop the future of dental materials science.

Molecular dynamics (MD) simulations

In this section, we discuss MD simulations, which is a key part of the study strategy to get an insight into the dynamic behavior and evolving intermolecular dynamics of dental resin composites. MD simulations provide the means to understand how these materials will evolve under dynamic loads and reveal their biomechanical and structural properties over time. This MD simulation was designed to explore the biomechanical behavior of dental composite complexes in terms of Young's modulus, shear modulus, and flexural strength. Furthermore, hydrogen bonds (stabilizers of ligand-ligand complexes) formed the basic molecular dynamics of the composite systems. The simulations employed the Forcite module and COMPASS II force field to provide realistic intra- and intermolecular dynamics in dental composite complexes. This module and force field combination is well-suited for modeling the dynamic behavior of polymers and organic materials⁴⁵. The energy of all the dental composite complexes simulated in the docking process was initially minimized to meet the energy convergence criteria of 0.001 kcal/mol, representing the threshold for the change in energy between successive steps, and a total potential energy of 5105 kcal/mol, corresponding to the fully minimized energy of the entire system. These criteria ensured that the system reached a stable energy state before proceeding to the subsequent MD simulations. After that, it was then emulated in an NVT ensemble with specified parameters (particle number, system volume, temperature) for 50 ns. A further 50 ns simulation was performed with the NPT ensemble using particle number, system pressure, and temperature at 1.0 bar and 298 K (using the Nose-Hoover Thermostat-Langevin and Berendsen barostats), with varying damping constants. The dental composite was equilibrated in the NVT ensemble at 298 K following a 50 ns overrun. The equations of motion were integrated using the Verlet velocity integration algorithm with a time step of 1 femtosecond (fs) for each simulation step. Strict calculation quality was selected for computational efficiency. Van der Waals and electrostatic interactions were calculated using the particle mesh Ewald method⁴⁶, allowing precise long-range electrostatic interactions. The resultant equilibrium molecular architecture of the dental resin composite created through MD simulations was used as input to subsequent structural and mechanical investigations. However, the COMPASS force field is widely recognized for its ability to model a broad range of molecular interactions, including van der Waals forces, electrostatic interactions, and bond stretch, which are crucial for understanding the mechanical properties of composites. While it does not include explicit hydrogen-bonding terms, COMPASS can still account for hydrogen bonds indirectly through its electrostatic and van der Waals interactions, which influence the overall stability and interaction of the components. Furthermore, in our study, we observed that hydrogen bonds were likely to form in the initial stages of complex formation, as the ligands and graphene-based materials come into contact. These hydrogen bonds were considered stabilizing interactions that supported the overall stability of the system during the simulation. Thus, although explicit hydrogen-bonding terms are not part of COMPASS, the force field remains a suitable choice for studying the composite material's mechanical properties and interactions, given its comprehensive representation of intermolecular forces. A total of 100 frames were used to calculate the mechanical properties and the number of hydrogen bonds in the simulations.

Results

Structural and energy minimization of monomers and graphene-based dental adhesives

Table 3 Table 3 illustrates a detailed comparison of energetic parameters between high-purity graphene and its diverse variations after MM2 energy minimization. This careful structure and energy minimization was a key ingredient in explaining how these molecules hold up and how they behave at the molecular level, revealing something fundamental about their possibilities as dental adhesives. High-purity graphene was a reliable candidate, and its energies had relatively low values for all parameters. This stability was confirmed by a previous paper which highlighted the strength of graphene's molecular framework because of its peculiar two-dimensional lattice structure⁴⁷. High-purity graphene had the highest values for stretch, bend, and 1,4 Van der Waals (VDW) interactions, indicating an efficient and energetically useful molecular structure.

On every parameter, GO and rGO were by far more energy-rich than high-purity graphene. This finding was similar to what Park et al. had discovered in GO (higher scalability, higher molecular asymmetry due to oxygen functional groups) and rGO (reduction mechanism)⁴⁸. In nitrogen-doped graphene, energy values varied from being at a neutral point – indicating that nitrogen doping provided structural rigidity but still was stable in general. This result has contended with another paper, which emphasized nitrogen doping in favor of improved mechanical and ductility of graphene-based materials⁴⁹. Fluorine-doped graphene also showed increased energy (stretch and bend parameters) that equated to greater molecular stretch and distortion. Sulfur-coated graphene was ambiguous in its energy content, containing many energies at different scales. This was in accordance with Yang et al.'s study describing multiple effects of sulphur doping on the crystalline and electronic structure of graphene and its ability to change material behaviour⁵⁰. The energy content of graphene quantum dots was medium, implying a molecular arrangement that is flexible and stable. This was also revealed by a study on the unique nature and applications of graphene quantum dots in many applications, from biomedicine to energy storage⁵¹. NH₂ functionalized graphene had lower energy values compared to high-purity graphene, suggesting that amine functionalization retained the stability of the graphene lattice but created special interaction points. COH and CCOOH functionalized graphene have different energy configurations, and COH shows less total energy and better stretch and bend parameters. Meanwhile, CCOOH showed high energies across most parameters, which implies structural instability. So, the energy minimization results provided insights into the structural robustness and malleability of graphene and its changes, as well as an avenue for further studies of their interactions with dental adhesive monomers and how they affect the properties of composites.

Molecular docking simulations of monomer and graphene-based dental adhesive complexes

This research phase involved the use of molecular docking simulations to probe and explore how monomers can interact with graphene-based dental adhesives, the basic building blocks of dental material assemblies. These simulations primarily targeted the testing of parameters such as the HADDOCK score (a.u.), binding energy, van der Waals energy, electrostatic energy, and desolvation energy for various combinations of the components. This molecular docking simulations allowed us to learn the stability and binding of monomer-graphene dental adhesive complexes key parameters for the design and performance of dental composites. Simulating the energetics and interactions of these fundamental components provided a more subtle explanation of their suitability and application in dental materials. Table 4 contains the results of the molecular docking simulations, such as binding energy and individual energy units given in kcal/mol (kcal/mol). Such values were calculated systematically as a guide to the complexity of the molecular interactions of any given combination. The results from docking showed significant differences in binding energies between the different monomer-graphene-based dental adhesive complexes. These differences represent the different interplay between the constituent parts and their suitability for dental alloys. In particular, some combinations had preferential binding energies compared to others, which indicates that they are well-suited for the construction of monomer-graphene interactions with superior performance. This full molecular docking simulation is provided in Supplementary Data 1.

The molecular docking simulations yielded extremely favorable monomer-graphene structures, with all combinations being associated with Root Mean Square Deviation (RMSD) less than 2.0. Notably, almost 90% of these combinations had RMSD less than 0.8, which shows high structural overlap between the predicted and best conformations. Figure 1a shows how the HADDOCK score and RMSD are correlated. In this context,

Structure	Stretch	Bend	Stretch-Bend	Torsion	Non-1,4 VDW	1,4 VDW	Total Energy (kcal/mol)
High-Purity Graphene	5.098	3.173	0.123	-165.458	-11.667	110.020	-58.710
Graphene Oxide (GO)	566.126	420.514	-20.856	323.780	602.940	317.374	2209.879
Reduced Graphene Oxide (rGO)	631.345	775.620	-39.638	433.057	509.372	412.552	2722.309
Nitrogen-doped Graphene	9.341	21.029	0.236	-74.801	-2.903	106.955	66.953
Fluorine-doped Graphene	324.172	983.567	-5.558	280.435	419.107	132.248	2133.973
Sulfur-doped Graphene	86.922	1503.161	-37.279	103.188	-6.753	135.782	1787.181
Graphene Quantum Dot	159.045	272.033	-0.403	70.054	82.269	188.230	771.229
NH ₂ Functionalized Graphene	8.879	22.195	0.197	-129.026	-2.733	109.129	8.704
COH Functionalized Graphene	7.851	14.181	0.054	-154.853	-11.379	103.407	-40.558
CCOOH Functionalized Graphene	15.578	33.394	0.579	-51.459	15.810	116.980	164.901

Table 3. Comparison of energetic parameters between high-purity graphene and its modifications following MM2 energy minimization.

Monomer	Graphene-based dental adhesive	HADDOCK score (a.u.)	Binding energy (kcal/mol)	Van der Waals energy	Electrostatic energy	Desolvation energy
Bis-GMA	High-Purity Graphene	-20.5 +/- 0.4	-6.28	-14.3 +/- 0.4	0.3 +/- 0.2	-6.2 +/- 0.1
	Graphene Oxide (GO)	-21.9 +/- 0.3	-6.51	-15.6 +/- 0.2	-28.6 +/- 4.3	-3.4 +/- 0.7
	Reduced Graphene Oxide (rGO)	-20.6 +/- 0.2	-6.22	-15.2 +/- 0.2	-3.6 +/- 0.4	-5.1 +/- 0.1
	Nitrogen-doped Graphene	-16.9 +/- 0.4	-6.19	-10.2 +/- 0.2	-49.7 +/- 2.5	-1.8 +/- 0.3
	Fluorine-doped Graphene	-20.4 +/- 0.1	-6.17	-14.6 +/- 0.2	-2.8 +/- 0.4	-5.6 +/- 0.3
	Sulfur-doped Graphene	-14.8 +/- 0.7	-6.15	-8.7 +/- 0.6	-40.8 +/- 5.2	-2.1 +/- 0.3
	Graphene Quantum Dot	-24.5 +/- 0.4	-6.67	-18.4 +/- 0.4	-14.9 +/- 0.2	-4.7 +/- 0.2
	NH ₂ Functionalized Graphene	-20.9 +/- 0.4	-6.32	-14.6 +/- 0.5	-4.2 +/- 0.3	-5.9 +/- 0.3
	COH Functionalized Graphene	-20.7 +/- 0.1	-6.28	-14.7 +/- 0.2	0.1 +/- 0.3	-6.1 +/- 0.2
	CCOOH Functionalized Graphene	-22.6 +/- 0.3	-6.65	-15.0 +/- 0.2	-26.2 +/- 1.4	-5.0 +/- 0.2
EBPADMA	High-Purity Graphene	-19.1 +/- 0.2	-6.10	-14.3 +/- 0.1	0.2 +/- 0.0	-4.8 +/- 0.2
	Graphene Oxide (GO)	-19.5 +/- 0.8	-6.14	-14.5 +/- 0.7	-2.0 +/- 1.9	-4.8 +/- 0.1
	Reduced Graphene Oxide (rGO)	-18.1 +/- 0.2	-6.01	-13.6 +/- 0.2	2.0 +/- 0.3	-4.8 +/- 0.1
	Nitrogen-doped Graphene	-18.2 +/- 0.1	-6.29	-11.4 +/- 0.2	-40.6 +/- 2.3	-2.7 +/- 0.1
	Fluorine-doped Graphene	-18.6 +/- 0.3	-6.02	-14.2 +/- 0.2	-0.3 +/- 0.2	-4.4 +/- 0.2
	Sulfur-doped Graphene	-14.8 +/- 0.9	-6.26	-8.9 +/- 0.9	-31.6 +/- 1.9	-2.8 +/- 0.2
	Graphene Quantum Dot	-21.9 +/- 0.3	-6.48	-16.4 +/- 0.2	-12.2 +/- 0.5	-4.3 +/- 0.1
	NH ₂ Functionalized Graphene	-19.0 +/- 0.4	-6.21	-14.1 +/- 0.2	-4.6 +/- 1.0	-4.4 +/- 0.4
	COH Functionalized Graphene	-19.2 +/- 0.1	-6.12	-14.8 +/- 0.2	0.7 +/- 0.1	-4.4 +/- 0.2
	CCOOH Functionalized Graphene	-21.2 +/- 0.2	-6.45	-15.7 +/- 0.4	-22.8 +/- 2.0	-3.2 +/- 0.2
HEMA	High-Purity Graphene	-11.4 +/- 0.3	-5.36	-9.9 +/- 0.1	0.3 +/- 0.1	-1.5 +/- 0.2
	Graphene Oxide (GO)	-13.3 +/- 0.3	-5.55	-9.9 +/- 0.3	-16.9 +/- 3.3	-1.7 +/- 0.2
	Reduced Graphene Oxide (rGO)	-11.7 +/- 0.1	-5.36	-9.6 +/- 0.2	-3.5 +/- 1.7	-1.7 +/- 0.1
	Nitrogen-doped Graphene	-13.4 +/- 0.2	-5.84	-7.8 +/- 0.2	-44.0 +/- 1.9	-1.2 +/- 0.0
	Fluorine-doped Graphene	-12.2 +/- 0.2	-5.36	-10.3 +/- 0.3	-2.9 +/- 0.6	-1.6 +/- 0.1
	Sulfur-doped Graphene	-11.0 +/- 0.2	-5.74	-5.5 +/- 0.3	-38.9 +/- 5.3	-1.6 +/- 0.3
	Graphene Quantum Dot	-11.9 +/- 0.3	-5.48	-9.8 +/- 0.3	-4.0 +/- 0.4	-1.7 +/- 0.1
	NH ₂ Functionalized Graphene	-12.3 +/- 0.5	-5.39	-10.3 +/- 0.3	-1.8 +/- 1.0	-1.8 +/- 0.3
	COH Functionalized Graphene	-12.0 +/- 0.4	-5.39	-10.2 +/- 0.2	-1.7 +/- 0.1	-1.7 +/- 0.1
	CCOOH Functionalized Graphene	-13.0 +/- 0.3	-5.49	-10.3 +/- 0.5	-8.9 +/- 2.6	-1.8 +/- 0.1
TEGDMA	High-Purity Graphene	-15.1 +/- 0.2	-5.63	-11.7 +/- 0.3	2.1 +/- 0.1	-3.6 +/- 0.2
	Graphene Oxide (GO)	-19.1 +/- 0.1	-6.09	-12.0 +/- 0.1	-46.5 +/- 1.2	-2.5 +/- 0.2
	Reduced Graphene Oxide (rGO)	-14.6 +/- 0.1	-5.57	-11.0 +/- 0.1	3.0 +/- 0.3	-3.9 +/- 0.0
	Nitrogen-doped Graphene	-16.8 +/- 0.0	-6.07	-9.6 +/- 0.2	-52.6 +/- 2.0	-2.0 +/- 0.1
	Fluorine-doped Graphene	-15.3 +/- 0.0	-5.62	-11.9 +/- 0.1	-2.9 +/- 0.6	-3.1 +/- 0.2
	Sulfur-doped Graphene	-13.1 +/- 0.3	-5.98	-6.4 +/- 0.6	-45.8 +/- 6.2	-2.1 +/- 0.3
	Graphene Quantum Dot	-17.6 +/- 0.2	-5.80	-13.8 +/- 0.2	-0.6 +/- 3.5	-3.7 +/- 0.2
	NH ₂ Functionalized Graphene	-16.4 +/- 0.1	-5.76	-12.6 +/- 0.2	-7.9 +/- 1.6	-3.1 +/- 0.1
	COH Functionalized Graphene	-15.3 +/- 0.1	-5.62	-12.4 +/- 0.1	2.9 +/- 0.4	-3.2 +/- 0.2
	CCOOH Functionalized Graphene	-17.4 +/- 0.2	-5.95	-12.3 +/- 0.4	-30.7 +/- 2.4	-2.1 +/- 0.1
UDMA	High-Purity Graphene	-17.5 +/- 0.1	-5.86	-13.2 +/- 0.3	1.4 +/- 0.1	-4.4 +/- 0.3
	Graphene Oxide (GO)	-19.8 +/- 0.4	-6.09	-13.7 +/- 0.1	-38.8 +/- 2.6	-2.2 +/- 0.3
	Reduced Graphene Oxide (rGO)	-16.7 +/- 0.9	-5.77	-11.9 +/- 1.0	4.1 +/- 0.9	-5.1 +/- 0.1
	Nitrogen-doped Graphene	-18.4 +/- 0.1	-6.04	-11.7 +/- 0.5	-44.7 +/- 3.4	-2.2 +/- 0.2
	Fluorine-doped Graphene	-17.8 +/- 0.1	-5.82	-13.5 +/- 0.0	-1.2 +/- 1.3	-4.2 +/- 0.1
	Sulfur-doped Graphene	-15.8 +/- 0.5	-6.03	-9.2 +/- 0.7	-41.9 +/- 2.0	-2.4 +/- 0.1
	Graphene Quantum Dot	-22.7 +/- 0.5	-6.23	-16.5 +/- 0.6	-17.1 +/- 1.2	-4.4 +/- 0.3
	NH ₂ Functionalized Graphene	-18.9 +/- 0.4	-5.88	-14.2 +/- 0.5	-1.0 +/- 0.8	-4.6 +/- 0.1
	COH Functionalized Graphene	-17.6 +/- 0.3	-5.87	-13.7 +/- 0.1	2.2 +/- 0.3	-4.1 +/- 0.4
	CCOOH Functionalized Graphene	-21.4 +/- 0.2	-6.44	-14.7 +/- 0.1	-46.9 +/- 2.1	-2.0 +/- 0.1

Table 4. Molecular Docking simulation results of monomer and graphene-based dental adhesive complexes. The shaded area denotes the optimal combination.

RMSD represents the difference between the predicted and optimal forms of the monomer-graphene complexes. The graph shows how changes in the HADDOCK score (binding affinity) are related to variations in the structural similarity of the predicted and ideal conformations (RMSD values). The smaller the RMSD values, the closer the predicted and optimal conformations were aligned and, thus, the better predictions of binding interactions^{52,53}. This correlation suggests the robustness of the docking simulations in making good predictions on the monomer-graphene interactions. As seen in Fig. 1b, the Pearson correlation between the HADDOCK score and binding affinity was high ($r=0.934$). This coefficient indicated a strong positive correlation between these two variables. Our high coefficient of correlation around one implied a very linear relationship between the HADDOCK score and the binding affinity of the monomer-graphene complexes. As the HADDOCK score increased (higher binding affinity), the binding affinity increased as well. Conversely, the lower the HADDOCK score (lower binding affinity), the lower the binding affinity. This correlation was also a sign that the HADDOCK scoring system could reliably and accurately predict the binding specificity of the monomer-graphene complexes. It highlighted how the computer-based predictions remained consistent with experimental results, giving reason to trust the molecular docking technique used in this study.

The binding affinities varied widely between monomer-graphene pairings in our data. Binding energy can be determined, which gives us the thermodynamic stability of monomer-graphene bonds. Figure 1c), where the best monomer-graphene pairs per monomer were presented, and the binding energy value with the lowest binding energies was interpreted as an indicator of greater adhesion. Bis-GMA's most effective preparation was adsorption on Graphene Quantum Dot (GQD) with binding energy -6.67 kcal/mol and HADDOCK score -24.5 . The pair also demonstrated high van der Waals energies (-18.4 kcal/mol) and high electrostatic energy (-14.9 kcal/mol), suggesting a very high binding affinity and stability, which concurs with other studies that have revealed that graphene quantum dots do better in composite materials because of their larger surface area and different electronic properties^{54,55}. These patterns were like what we had with Bis-GMA complexes but for EBPADMA with graphene. It should be mentioned that the best interaction occurred with GQD (binding energy: -6.48 kcal/mol; HADDOCK score: -21.9). It was a complex mixture of strong van der Waals effects (-16.4 kcal/mol) and strong electrostatic effects (-12.2 kcal/mol). That demonstrates GQD's robustness as an attractive solution for the enhancement of adhesive properties on monomer systems. Nitrogen-doped Graphene offered the most suitable match to HEMA (binding energy -5.84 kcal/mol; HADDOCK score -13.4). This combination was especially electrostatically active (-44.0 kcal/mol), which was crucial to the formation of permanent bonding on dental adhesives. However, nitrogen doping of graphene has also been found to dramatically enhance its electronic characteristics and enable it to interact with other molecules^{56,57}. TEGDMA had the best interaction with GO (binding energy -6.09 kcal/mol and HADDOCK score of 19.1). The combination had both effective van der Waals forces (-12.0 kcal/mol) and strong electrostatic effects (-46.5 kcal/mol). Graphene oxide has long been shown to increase the mechanical properties of composites as its high surface area and functional groups provide strong interactions with the polymer matrix⁵⁸. Lastly, the CCOOH Functionalized Graphene combination was the most favorable pairing for UDMA (binding energy -6.44 kcal/mol; HADDOCK score -21.4). This interaction possessed high van der Waals forces (-14.7 kcal/mol) and large electrostatic forces (-46.9 kcal/mol), representing a stable and strong bond. Similar research has shown that functionalized graphene compounds such as CCOOH can improve the dispersion and interaction with the polymer matrix and produce better composites^{59,60}.

Figure 1d shows a correlation matrix, a graph describing the relationship between the binding energy and individual energies – van der Waals energy, electrostatic energy, and desolvation energy. This matrix was a great analytical tool for understanding how these energy factors interacted with each other in monomer-graphene adhesive complexes. The Pearson correlation coefficient quantifies the relationship between the binding energy (kcal/mol) and its components, including van der Waals energy, electrostatic energy, and desolvation energy. The Pearson correlation coefficient is calculated using the following formula:

$$r = \frac{n(\sum xy) - (\sum x)(\sum y)}{\sqrt{[n\sum x^2 - (\sum x)^2][n\sum y^2 - (\sum y)^2]}}$$

Where:

- x and y represent the individual energy components (e.g., van der Waals, electrostatic, or desolvation).
- n is the number of data points (i.e., number of systems in this case).
- The summations are taken over all the data points for each energy component.

In the correlation matrix, there was a correlation coefficient for each cell. This measure of numbers defined the strength and direction of correlation between two variables — in this case, the binding energy and each element of energy. These coefficients were between -1 and 1 , where in-between was a positive correlation, zero was a negative correlation, and near zero was a very slight correlation. A correlation coefficient of 1 indicated a perfect positive correlation (that is, the increase in one perfectly replicated the increase in the other). A coefficient of -1 , on the other hand, represented a perfect negative correlation: drops precisely balance increases in one variable. If the coefficient was 0 , it meant there was no linear interaction between variables. The correlation coefficients were analyzed, revealing interesting facts about the mechanism of monomer-graphene adhesive interaction. For example, the positive correlation coefficient of van der Waals energy ($r=0.60$) predicted that greater van der Waals energy correlated to higher binding energy. It amounted to the finding that van der Waals interactions were critical for stabilizing the complexes, which in turn were responsible for their overall stability and stickiness. Van der Waals interactions, a form of non-covalent binding between atoms or molecules, occur because of changes in electron distribution among particles. Such interactions are especially significant in contexts where molecules are remarkably close to each other without forming chemical bonds^{61,62}. In monomer-

graphene adhesive complexes, van der Waals forces may be important to enable the two components to become tightly bound and bond, thereby enhancing both stability and adhesion. Van der Waals interactions hold the complexes together with attractive forces between the molecules involved, making the entire system adhesive. This stabilization is vital to the health and long-term performance of the restoration, as it averts the peeling or crumbling of the adhesive interface under a wide range of stresses encountered in the mouth.

Likewise, the positive correlation of electrostatic energy ($r=0.37$) suggested that electrostatic interactions also helped to stabilize the complexes, but to a slightly weaker degree than van der Waals interactions. That meant that electrostatic forces had a part to play in adhesion, but perhaps slightly less than van der Waals forces. Electrostatic interactions are caused by a charge-attracting or repelling relationship between charged ions or polar molecules and depend on the charges present in molecules^{63,64}. With monomer-graphene adhesive complexes, the electrostatic forces are likely to be caused by the charge/polar functional groups present in the monomers and the surfaces of graphene. These interactions are part of what makes the complexes stick together overall by allowing the pieces to get close together. The slightly higher correlation coefficient of desolvation energy ($r=0.50$) complemented this fact that the desolvation reaction played a crucial role in maintaining the stability of monomer-graphene adhesive complexes. The energy required for the desolvation is the removal of solvent molecules from the contact area between the monomers and graphene⁶⁵. This correlation suggests that the desolvation energy is actually a key factor in the overall bonding capacity of the complexes. Desolvation enables close contact between the monomers and graphene surfaces because molecules of the solvent interfere with efficient molecular interaction. Desolvation eliminates the solvent molecules from the interface, which in turn creates strong intermolecular bonds between the monomers and graphene, improving the complexes' stability and adhesiveness^{66,67}.

Molecular dynamics simulations for the best combinations of monomers and graphene-based dental adhesive

As a step towards figuring out how graphene dental adhesives affect the mechanical properties of dental composites, MD simulations were performed to evaluate the mechanical properties of optimal monomer and graphene dental adhesive mixtures. These simulations reveal the atomic-scale relationships between these elements and how they translate to performance in dental composites.

Young's modulus (E)

Young's modulus, a measure of material stiffness, was estimated from MD stress-strain simulations, where the system was subjected to uniaxial tensile deformation. The stress-strain response was extracted by gradually applying tensile strain and measuring the corresponding stress, ensuring that the elastic region was captured for modulus calculations. The obtained modulus values were then compared with theoretical estimations based on the rule of mixtures:

$$E = \sum_{i=1}^n f_i \cdot E_i \quad (1)$$

Where:

- E is the estimated Young's modulus of the system,
- f_i is the volume fraction of component ,
- E_i is the Young's modulus of component ,
- i represents the individual components within the system (the monomer and the graphene-based material), and
- n is the total number of components considered in the mixture.

In this study, the monomer and graphene-based material are the two primary components ($i = 1$ corresponds to the monomer, and $i = 2$ corresponds to the graphene-based material). The volume fraction (f_i) of each component was determined based on the atomic composition in the simulation system. However, it is important to note that while the rule of mixtures provides a theoretical framework for estimating composite stiffness, its direct application assumes a fully developed polymeric structure. Since our study employs monomer-based models rather than polymeric chains, the MD simulations primarily provide insights into atomic-scale interactions rather than exact bulk mechanical properties of the final dental composite. Thus, the Young's modulus derived from MD stress-strain simulations reflects the molecular-level behavior of the monomer-graphene system, rather than predicting the final stiffness of a polymerized dental adhesive. The rule of mixtures was referenced to conceptually understand stiffness variation trends rather than serve as a precise mechanical property predictor.

Shear modulus (G)

Likewise, the shear modulus (which measures how much a material resists deformation under shear stress) was calculated from the rule of mixtures. This calculates the shear modulus of the composite by considering the volume fractions and shear moduli of the composite parts. Through measurement of shear modulus, MD simulations allowed for the comparison of the effects of graphene-based adhesives on the composites' shear strength.

$$G = \frac{1}{2} \sum_{i=1}^n f_i \cdot G_i \quad (2)$$

Where:

- G is the shear modulus of the composite.
- f_i is the volume fraction of the component i .
- G_i is the Shear modulus of the component i .

Flexural strength

Moreover, the flexibility of the dental composite was measured to know its resistance to bending or flexing. The estimation of flexural strength was based on a formula for tensile and compressive strengths. By measuring the flexural strength, the simulations revealed how the combination of tensile and compressive stress affected the overall mechanical strength of the composite.

$$\sigma_{flexural} = \sqrt{\sigma_{tensile} \cdot \sigma_{compressive}} \quad (3)$$

Where:

- $\sigma_{flexural}$ is the flexural strength.
- $\sigma_{tensile}$ is the tensile strength.
- $\sigma_{compressive}$ is the compressive strength.

Figure 2; Table 5 show the mechanical stability of the best monomer-graphene complexes from MD simulations. These include Young's modulus, shear modulus, flexural strength, and hydrogen bond numbers, which tell us anatomically how these composites will behave.

Young's modulus of the monomer-graphene complexes was also high, suggesting different stiffness in the composites. This difference is important as it directly impacts the mechanical stability and utilization of the composites for various dental functions. The Bis-GMA-Graphene Quantum Dot structure had the highest Young's modulus (14.74 GPa) and was, therefore, more rigid and less deformation-resistant under stress. These results suggest that Bis-GMA and graphene quantum dots could be structurally strong and stable, making them ideal for high-strength stability materials for load-bearing applications such as tooth restoration. Prior to the Bis-GMA-Graphene Quantum Dot, the EBPADMA-Graphene Quantum Dot complex demonstrated Young's modulus of 14.28 GPa, and the UDMA-CCOOH Functionalized Graphene complex was 13.82 GPa. These extremely high Young's modulus values correlate with the massive increase in stiffness due to the graphene quantum dots and functionalized graphene. The composites will be strong enough to resist mechanical wear, creating durable, long-lasting dental restorations. The HEMA-Nitrogen-strengthened Graphene complex, however, presented the lowest Young's modulus (9.85 GPa). That lower stiffness means the composite is soft and less rigid than the others. That might be a downfall in certain circumstances but can be a benefit in some dental situations that require a certain degree of flexibility. For example, where it needs to withstand small morphological changes and mouth loads without shattering or delamination, a less rigid material like HEMA-Nitrogen-based Graphene can work best.

The shear modulus – which reflects the resistance of the material to shear stress – was almost identical to Young's modulus for all monomer-graphene complexes. This stability underlines the strong mechanical capabilities of some combinations, making them viable for complex dental needs. The bis-GMA-Graphene Quantum Dot complex had the highest shear modulus (9.32 GPa). It's the ratio that defines its rigidity, which means that the composite is exceptionally resistant to shear deformation. This is extremely helpful in dental restorations that require lateral stress (when chewing and grinding)⁶⁸. The high shear strength of the Bis-GMA-Graphene Quantum Dot complex allows for greater stability and durability when applied to high-stress dentistry. EBPADMA-Graphene Quantum Dot complex, followed by an 8.43 GPa shear modulus and UDMA-CCOOH Functionalized graphene complex. These higher values also confirm their use for applications where there is high shear stress. The graphene quantum dots and functionalized graphene present in these composites allow these composites to have huge shear strength, enabling them to stay stable and efficient with mechanical loads.

Conversely, the HEMA-Nitrogen-doped Graphene complex showed the lowest shear modulus of 6.86 GPa. The lower number corresponds to its lower Young's modulus, which indicates a more flexible substance with both compressive and shear loads. This may mean less rigidity but also more flexibility. The more flexible properties of the HEMA-Nitrogen-doped Graphene complex might help dental applications, where materials must absorb and resist various forces and need flexibility. This flexibility can reduce stress concentrations and, thus, the chances of material failure with complex loads.

The flexibility strength, one of the main properties of dental composites, determines the material's tenacity in response to bending forces⁶⁹. That is a particularly important aspect in dental applications where materials are required to withstand repeated, dynamic mechanical stress. Out of the 57 complexes investigated, the Bis-GMA-Graphene Quantum Dot complex exhibited the highest flexural resistance of 120.51 MPa. This level of flexural strength means this composite is exceptionally durable when subjected to intense amounts of bending stresses, which makes it the perfect choice for dental restorations and fillings that require mechanical toughness. This higher flexural strength makes the Bis-GMA-Graphene Quantum Dot composite suitable for preserving integrity and functionality under long-term, extreme loading. Following closely on the heels of this, the EBPADMA-Graphene Quantum Dot complex achieved a flexural strength of 118.22 MPa and the UDMA-CCOOH Functionalized graphene complex at 115.4 MPa. These high values prove the dental applications of these composites for applications requiring high resistance to bending. Graphene quantum dots and functional graphene give these composites a general more mechanical advantage that ensures durability under harsh conditions.

Both the TEGDMA-Graphene Oxide complex (110.23 MPa) and HEMA-Nitrogen-doped Graphene complex (95.7 MPa) were also able to resist the bending. While these figures are inferior to the super-success complexes,

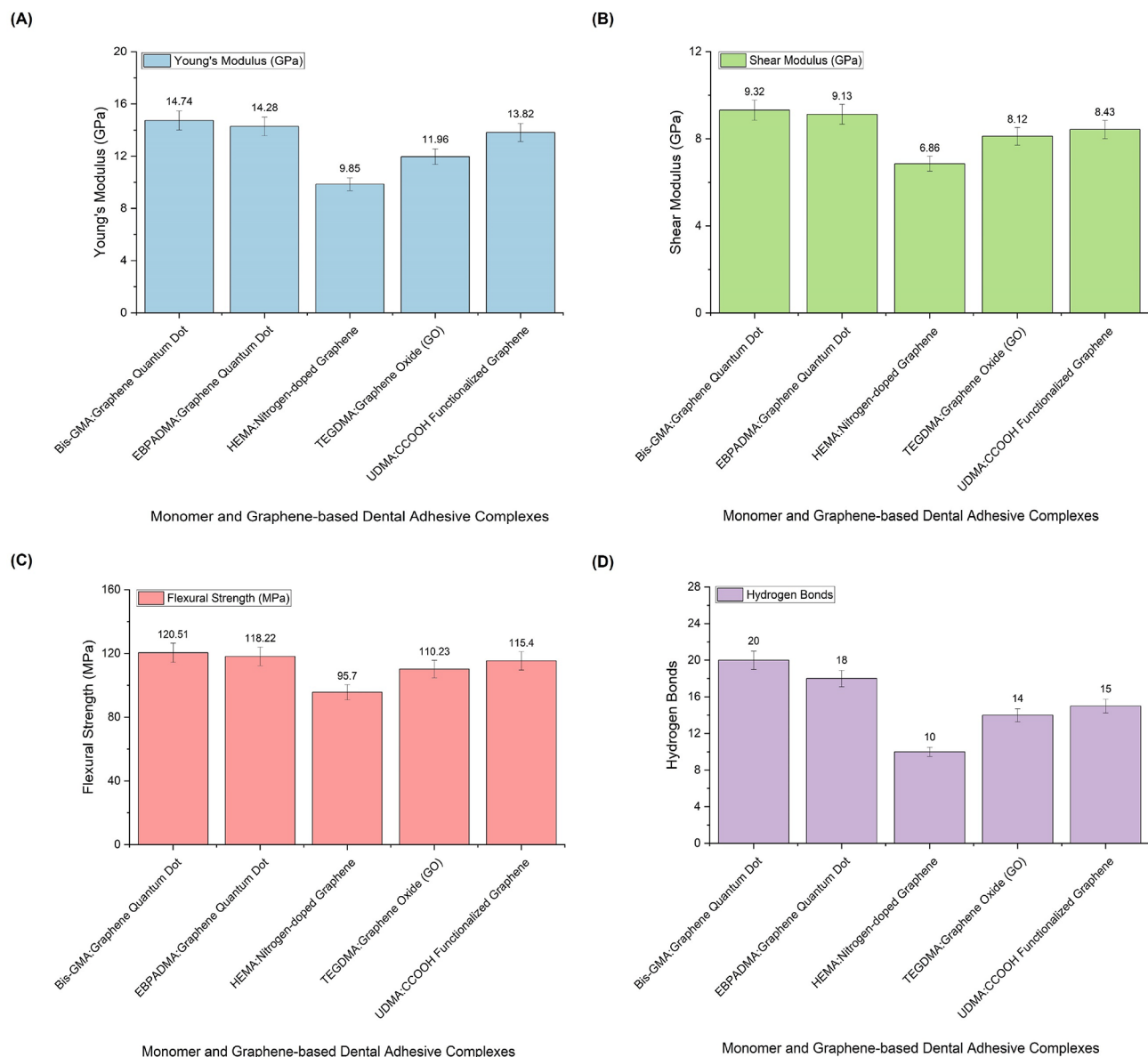


Fig. 2. Molecular dynamics simulation results for the best dental composite complex. **(A)** Young's modulus (GPa). **(B)** Shear modulus (GPa). **(C)** Binding strength (MPa). **(D)** Hydrogen bonds.

Monomer-Graphene Complex	Young's Modulus (GPa)	Shear Modulus (GPa)	Flexural Strength (MPa)	Hydrogen Bonds
Bis-GMA-Graphene Quantum Dot	14.74	9.32	120.51	20
EBPADMA-Graphene Quantum Dot	14.28	9.13	118.22	18
HEMA-Nitrogen-doped Graphene	9.85	6.86	95.7	10
TEGDMA-Graphene Oxide (GO)	11.96	8.12	110.23	14
UDMA-CCOOH Functionalized Graphene	13.82	8.43	115.4	15

Table 5. Mechanical properties of monomer-graphene complexes in dental composite materials: insights from MD simulation.

this still hints at high flexural strength. What comes out of it is that these composites are used in dentistry for medium to high bending loads. TEGDMA-Graphene Oxide complex, especially, is a unique combination of mechanical properties and is suitable for all sorts of dental applications. The HEMA-Nitrogen-doped Graphene complex has extremely poor flexural strength and is not suitable for high loads, but it provides satisfactory

results in mild bending applications. Lower flexural stiffness gets compensated for in some cases through its more elasticity and sturdiness, which may help with certain dental restorations that need to be flexible.

The number of hydrogen bonds in the complexes gives us a measure of intermolecular connectivity and the overall stability of the composites. By imparting added binding forces between components, hydrogen bonds can provide mechanical strength and stability to composites^{28,70}. The Bis-GMA-Graphene Quantum Dot complex in this experiment had the most hydrogen bonds, which reached 20. Such high numbers of hydrogen bonds are why it has so many good mechanical features, such as its impressive Young's modulus, shear modulus, and flexural strength. With all those hydrogen bonds, there is likely a lot of interaction between molecules that gives the composite good strength and rigidity and makes it extremely resistant to mechanical strains. EBPADMA-Graphene Quantum Dot complex, with 18 hydrogen bonds, also exhibited good intermolecular interactions. This high density of hydrogen bonds shows up in its mechanical composition, which closely resembles the Bis-GMA-Graphene Quantum Dot complex. The substantial number of hydrogen bonds in this complex probably contributes to its high Young's modulus and shear modulus, signifying the rigid and shear-resistant nature of the structure. Likewise, the UDMA-CCOOH Functionalized Graphene complex (15 hydrogen bonds) exhibits robust intermolecular interactions required for mechanical strength. The hydrogen bonds add to the strength of the composite, making it robust in terms of mechanical characteristics, including its Young's modulus, shear modulus, and flexural strength. The HEMA-Nitrogen-doped Graphene complex, on the other hand, had fewer hydrogen bonds (10 in total). This small amount of hydrogen bonds might be attributed to its small mechanical stiffness, like Young's modulus and shear modulus. The fewer hydrogen bonds indicate weaker intermolecular forces, making the composite structure less stiff and flexible^{71,72}. This can be advantageous for flexible applications, but it also entails less resistance to mechanical stress. TEGDMA-Graphene Oxide complex (14 hydrogen bonds) had a small number of hydrogen bonds. This is not as high as the best complexes, but it still suggests a good amount of intermolecular interaction. Its moderate number of hydrogen bonds manifests in the mechanical properties, acceptable for many dental applications but below those of complexes that hold more hydrogen bonds.

Discussion

This work helped to provide a better understanding of the structural stability, molecular interaction, and mechanical behavior of graphene dental adhesives and their potential use for dental composites. These observations led to the continuous search for high-performance and long-lasting dental materials. The structural stability of graphene-based materials was essential to their suitability for dental use. We found that high-purity graphene had low energy values in various parameters, reflecting stability and stable molecular structure. This result was similar to the work by Li et al., who previously used density functional theory (DFT) calculations to estimate the stability of pristine graphene. Li et al. concluded that pristine graphene has a very stable structure because of its sp² hybridization and plane structure (which also matches our finding⁷³). Instead, graphene oxide (GO) and reduced graphene oxide (rGO) modifications exhibited more energy, corresponding to higher elasticity and molecular distortion. This increased energy corresponds to the additional molecular interactions, such as electrostatic and van der Waals forces, that result from the modifications. Regarding “higher elasticity,” we should clarify that we were referring to the increased flexibility and deformation capability of these modified graphene systems, as observed through the mechanical simulations (e.g., strain-stress behavior). Higher elasticity, in this context, indicates that GO and rGO composites showed greater ability to undergo deformation before failure, suggesting they might be more adaptable under mechanical stress. This was consistent with Chen et al. and Stankovich et al., who studied graphene structural modifications by oxygen functionalization and reduction^{74,75}. Chen et al. reported that oxygen-rich functional groups in GO form structural cracks and damage the sp² carbon network, causing increased flexibility and energy⁷⁴. In a similar vein, Stankovich et al. observed that GO reduction restores sp² hybridization while introducing structural disorder in the mechanical properties of rGO⁷⁵. The higher energy values observed for GO and rGO are attributed to the functionalization processes, which introduce oxygen-containing groups that disrupt the original graphene structure, leading to a loss of conjugation and increased flexibility. This increased flexibility allows for more interaction with the polymer matrix, enhancing the composite's overall mechanical performance. Our molecular docking and MD simulations suggest that such modifications in graphene's structure enhance its compatibility and interaction with the monomers, further improving the composite's mechanical properties. This behavior is in line with previous reports where modifications to graphene, such as doping or functionalization, were shown to improve the mechanical properties of polymer composites by improving the interfacial bonding between the graphene filler and the polymer matrix.

The molecular docking simulations demonstrated favorable binding energies and structural match between monomers and graphene-based dental adhesives in particular combinations. The association of HADDOCK score with binding affinity also confirmed the docking simulations' ability to predict the stability of monomer-graphene complexes. The simulations by molecular dynamics were also used to estimate Young's modulus, shear modulus, and flexural strength for the most optimal monomer-graphene complexes. Our findings were in agreement with Zhang et al. and Park et al., who examined the mechanical reinforcement performance of graphene-based materials in polymer composites^{76,77}. Zhang et al. reported significant increases in the stiffness and strength of epoxy composites containing graphene oxide based on the good interactions and uniform spread of graphene sheets⁷⁶. Cai et al. demonstrated the same mechanical improvements for polyurethane composites reinforced with well-dispersed graphene oxide, highlighting the additive role of graphene and polymer matrix⁷⁸.

Limitations and clinical considerations

A limitation of our study is the use of monomer-based models instead of polymer chains to represent graphene-based dental composites. While our approach allows for a fundamental understanding of monomer–graphene interactions, it does not fully capture polymerization effects such as chain entanglements, cross-linking, and bulk mechanical reinforcement. Therefore, while our results provide valuable insights into molecular-scale adhesion and stiffness trends, they should not be directly extrapolated to predict the mechanical properties of a fully polymerized dental composite. Future studies incorporating polymer chains will be necessary to refine our understanding and bridge the gap between molecular interactions and bulk material behavior. The simulations provide a convenient abstraction of the dynamics of molecules and materials yet are trivial to use in practice. This will require in vitro and in vivo studies to establish the efficacy, safety, and clinical applications of graphene dental adhesives. Another vulnerability is the simplifying models in the research. Machine-generated simulations can sometimes minimize the biological and mechanical complexity of tooth tissues and surfaces. These are good models to start studying, but more detailed models that can capture tissue variability and load regime change would be more accurate to simulate clinical realities. Second, material uniformity in simulations failed to account for the problems resulting from actual dispersion and graphene filler incorporation into resin matrices. In fact, this difference in the distribution of material and property features has real implications for material performance and clinical impact that require future exploration.

Moreover, it is not yet clear whether the graphene components will be biocompatible and cytotoxic. Although some studies suggest they can be used in dentistry, we still need to know about long-term biocompatibility and tissue responses. These problems need to be addressed through testing and regulatory approval prior to clinical trials. From a clinical perspective, regulatory approval is a big milestone for commercial graphene dental adhesives. We must adhere to industry requirements and regulations by rigorous testing and validation to ensure safety and efficacy in clinical trials. Also, clinical validation using clinically optimized research would enable the application of graphene dental adhesives to determine their efficacy, strength, and biocompatibility.

Such studies can be analyzed for important clinical decisions in terms of longevity, bond strength, and degrade stability. This is particularly important when it comes to the compatibility of graphene-based adhesives with other dental materials. Adaptability testing needs to be done to verify any interactions and make sure it is functioning at its best in the clinical setting.

Lastly, dentists also must be sensitive to patients' needs regarding dental hygiene, chronic illness, and aesthetic preference in tooth selection. Graphene adhesives should be studied for patients, as well as their treatment goals and clinical indications, including specific therapy.

Conclusion and future works

Overall, this research gives a detailed understanding of the structure and mechanical behavior of graphene-based dental adhesives and their applications in restorative dentistry. Computational modeling and simulation allowed us to clarify the molecular interactions, adhesion, and mechanical behavior of different monomer–graphene interactions. These results confirm that different combinations of graphene modification result in different effects on adhesive properties and that some combinations offer higher stability, adhesion, and mechanical properties. Specifically, graphene quantum dots and functionalized graphene compounds were attractive options to optimize the properties of monomer–graphene interactions through adhesive interfaces and improved mechanical properties. However, several areas of research and development need to be done to develop graphene dental adhesives further. For one, we need experimental validation of the computational predictions to confirm these materials' effectiveness and safety in clinical applications. Biocompatibility, cytotoxicity, and performance data are all required in vitro and in vivo to validate for regulatory approval and clinical application.

More realistic tissue shapes, loads, and distributions of materials would make the simulations more accurate and predictive, resulting in more informed material design and optimization. Furthermore, clinical trials to validate the effectiveness and safety of graphene dental adhesives in a wide variety of patients and clinical settings are also warranted. Extensive, longitudinal clinical trials of graphene-based adhesives and other materials would be needed to provide us with data on performance, resistance, and clinical efficacy, allowing for informed choices about restorative dentistry.

Data availability

Data supporting the findings of this study are available from the corresponding author upon reasonable request.

Received: 19 November 2024; Accepted: 7 March 2025

Published online: 19 March 2025

References

1. Alyahya, Y. A narrative review of minimally invasive techniques in restorative dentistry. *Saudi Dent. J.* **36** (2), 228–233 (2024).
2. Carvalho, R. M., Manso, A. P., Geraldini, S., Tay, F. R. & Pashley, D. H. Durability of bonds and clinical success of adhesive restorations. *Dent. Mater.* **28** (1), 72–86 (2012).
3. Baraka, M., Ibrahim, Y., Helmy, R., ADHESIVE STRATEGIES FOR RESTORING PRIMARY & AND YOUNG PERMANENT DENTITION-A REVIEW. *Alexandria Dent. J.* **49**:195–202. (2024).
4. Mousavinasab, S. M. Biocompatibility of composite resins. *Dent. Res. J. (Isfahan)*. **8** (Suppl 1), S21–S29 (2011).
5. Bertassoni, L. E., Habelitz, S., Marshall, S. J. & Marshall, G. W. Mechanical recovery of dentin following remineralization in vitro—an indentation study. *J. Biomech.* **44** (1), 176–181 (2011).
6. Stansbury, J. et al. Conversion-dependent shrinkage stress and strain in dental resins and composites. *Dent. Materials: Official Publication Acad. Dent. Mater.* **21**, 56–67 (2005).
7. Perdigão, J. Current perspectives on dental adhesion: (1) dentin adhesion - not there yet. *Jpn Dent. Sci. Rev.* **56** (1), 190–207 (2020).
8. Drummond, J. L. Degradation, fatigue, and failure of resin dental composite materials. *J. Dent. Res.* **87** (8), 710–719 (2008).

9. Mitra, S. B., Wu, D. & Holmes, B. N. An application of nanotechnology in advanced dental materials. *J. Am. Dent. Assoc.* **134** (10), 1382–1390 (2003).
10. Kusuma Yulianto, H. et al. Biofilm composition and composite degradation during intra-oral wear. *Dent. Mater.* **35**(5), 740–750. <https://doi.org/10.1016/j.dental.2019.02.024> (2019).
11. Tu, Y., Ren, H., He, Y., Ying, J. & Chen, Y. Interaction between microorganisms and dental material surfaces: general concepts and research progress. *J. Oral Microbiol.* **15** (1), 2196897 (2023).
12. Geim, A. K. & Novoselov, K. S. The rise of graphene. *62009*. pp. 11–9.
13. Walimbe, P. & Chaudhari, M. State-of-the-art advancements in studies and applications of graphene: a comprehensive review. *Mater. Today Sustain.* **6**, 100026 (2019).
14. Williams, A. G., Moore, E., Thomas, A. & Johnson, J. A. Graphene-Based materials in dental applications: antibacterial, biocompatible, and bone regenerative properties. *Int. J. Biomater.* **2023**, 8803283 (2023).
15. Mobarak, M. H. et al. Advances of graphene nanoparticles in dental implant applications – A review. *Appl. Surf. Sci. Adv.* **18**, 100470 (2023).
16. Hussein, A. H. & Yassir, Y. A. Graphene as a promising material in orthodontics: A review. *J. Orthod. Sci.* **13**, 24 (2024).
17. Alnatheer, M., Alqerban, A. & Alhazmi, H. Graphene Oxide-Modified dental adhesive for bonding orthodontic brackets. *Int. J. Adhes. Adhes.* **110**, 102928 (2021).
18. Sindi, A. Applications of graphene oxide and reduced graphene oxide in advanced dental materials and therapies. *J. Taibah Univ. Med. Sci.* **19**, 403–421 (2024).
19. Rygas, J., Matys, J., Wawrzyńska, M., Szymonowicz, M. & Dobrzyński, M. The use of graphene oxide in Orthodontics—A systematic review. *J. Funct. Biomater.* **14**(10), 500. <https://doi.org/10.3390/jfb14100500> (2023).
20. Li, Y. et al. Preparation of PDA-GO/CS composite scaffold and its effects on the biological properties of human dental pulp stem cells. *BMC Oral Health.* **24** (1), 157 (2024).
21. Syama, S. & Mohanan, P. V. Comprehensive application of graphene: emphasis on biomedical concerns. *Nano-Micro Lett.* **11** (1), 6 (2019).
22. Li, X. et al. Graphene-Based nanomaterials for dental applications: principles, current advances, and future outlook. *Front. Bioeng. Biotechnol.* **10**, 804201 (2022).
23. Roma, M. & Hegde, S. Implications of graphene-based materials in dentistry: present and future. *Front. Chem.* **11**, 1308948 (2023).
24. Vinagre, A. & Ramos, J. Adhesion in Restorative Dentistry. (2016).
25. Sofan, E. et al. Classification review of dental adhesive systems: from the IV generation to the universal type. *Ann. Stomatol. (Roma)*. **8** (1), 1–17 (2017).
26. Verma, A., Parashar, A. & Packirisamy, M. Effect of grain boundaries on the interfacial behaviour of graphene-polyethylene nanocomposite. *Appl. Surf. Sci.* **470**, 1085–1092 (2019).
27. Verma, A., Parashar, A. & Packirisamy, M. Atomistic modeling of graphene/hexagonal Boron nitride polymer nanocomposites: a review. *WIREs Comput. Mol. Sci.* **8** (3), e1346 (2018).
28. Saini, R. S. et al. Dental biomaterials redefined: molecular Docking and dynamics-driven dental resin composite optimization. *BMC Oral Health.* **24** (1), 557 (2024).
29. Ferracane, J. L. Resin composite—state of the Art. *Dent. Mater.* **27** (1), 29–38 (2011).
30. Apostu, A. M. et al. Can graphene pave the way to successful periodontal and dental prosthetic treatments? A narrative review. *Biomed.* **11**(9), 2354. <https://doi.org/10.3390/biomedicines11092354> (2023).
31. Ghosh, S. et al. Extremely high thermal conductivity of graphene: Prospects for thermal management applications in nanoelectronic circuits. *Appl. Phys. Lett.* **92**(15), 151911. <https://doi.org/10.1063/1.2907977> (2008).
32. Yadav, S. et al. An update on graphene oxide: applications and toxicity. *ACS Omega.* **7** (40), 35387–35445 (2022).
33. Konios, D., Stylianakis, M., Stratakis, E. & Kymakis, E. Dispersion behavior of graphene oxide and reduced graphene oxide. *J. Colloid Interface Sci.* **430**, 108–112 (2014).
34. Razmjooei, F., Singh, K., Song, M. & Yu, J.-S. Enhanced electrocatalytic activity due to additional phosphorous doping in nitrogen and sulfur-doped graphene: A comprehensive study. *Carbon* **78**, 257–267 (2014).
35. Wang, T., Wang, L. X., Wu, D. L., Xia, W. & Jia, D. Z. Interaction between nitrogen and sulfur in co-doped graphene and synergetic effect in supercapacitor. *Sci. Rep.* **5**, 9591 (2015).
36. Thangadurai, T. D., Manjubaashini, N., Nataraj, D., Gomes, V. & Lee, Y. I. A review on graphene quantum dots, an emerging luminescent carbon nanolights: healthcare and environmental applications. *Mater. Sci. Engineering: B.* **278**, 115633 (2022).
37. Chung, S., Revia, R. A. & Zhang, M. Graphene quantum Dots and their applications in bioimaging, biosensing, and therapy. *Adv. Mater.* **33** (22), e1904362 (2021).
38. Jha, S. et al. First-Principles study of the interactions between graphene oxide and Amine-Functionalized carbon nanotube. *J. Phys. Chem. C.* **122**, 1288–1298 (2017).
39. Gupta, B. et al. Role of oxygen functional groups in reduced graphene oxide for lubrication. *Sci. Rep.* **7**, 45030 (2017).
40. O’Boyle, N. M. et al. Open babel: an open chemical toolbox. *J. Cheminform.* **3** (1), 33 (2011).
41. Soo, G. C., Cartledge, F. K., Unwalla, J. & Profeta, R. Development of a molecular mechanics (MM2) force field for α -chlorosilanes. *Tetrahedron* **46** (24), 8005–8018 (1990).
42. Cousins, K. R. Computer review of ChemDraw ultra 12.0. *J. Am. Chem. Soc.* **133** (21), 8388 (2011).
43. Dominguez, C., Boelens, R. & Bonvin, A. M. J. J. HADDOCK: A Protein–Protein Docking approach based on biochemical or biophysical information. *J. Am. Chem. Soc.* **125** (7), 1731–1737 (2003).
44. Vangone, A. & Bonvin, A. M. J. J. PRODIGY: A Contact-based predictor of binding affinity in Protein-protein complexes. *Bio Protoc.* **7**(3), e2124. <https://doi.org/10.21769/BioProtoc.2124> (2017).
45. Sun, H. et al. COMPASS II: extended coverage for polymer and drug-like molecule databases. *J. Mol. Model.* **22** (2), 47 (2016).
46. Simmonett, A. C. & Brooks, B. R. A compression strategy for particle mesh Ewald theory. *J. Chem. Phys.* **154** (5), 054112 (2021).
47. Nan, H. et al. The thermal stability of graphene in air investigated by Raman spectroscopy. *J. Raman Spectrosc.* **44**, 1018–1021 (2013).
48. Park, S. et al. Graphene oxide papers modified by divalent ions-enhancing mechanical properties via chemical cross-linking. *ACS Nano.* **2** (3), 572–578 (2008).
49. Usachov, D. et al. Nitrogen-Doped graphene: efficient growth, structure, and electronic properties. *Nano Lett.* **11**, 5401–5407 (2011).
50. Yang, Z. et al. Sulfur-doped graphene as an efficient metal-free cathode catalyst for oxygen reduction. *ACS Nano.* **6** (1), 205–211 (2012).
51. Nesakumar, N., Srinivasan, S. & Alwarappan, S. Graphene quantum Dots: synthesis, properties, and applications to the development of optical and electrochemical sensors for chemical sensing. *Mikrochim. Acta.* **189** (7), 258 (2022).
52. Dermawan, D., Sumirtanurdin, R. & Dewantisari, D. Simulasi Dinamika Molekular reseptor Estrogen Alfa Dengan andrografolid Sebagai anti Kanker Payudara. *Indones J. Pharm. Sci. Technol.* **6** (2), 65–76 (2019).
53. Kufareva, I. & Abagyan, R. Methods of protein structure comparison. *Methods in molecular biology. (Clifton NJ)*. **857**, 231–257 (2012).
54. Alam, N., Ihsan, H., Khan, S. & Ullah, K. Graphene Quantum Dots-Based Composites for Biomedical Applications. pp. 62–90. (2024).

55. Sheikh Mohd Ghazali, S., Fatimah, I., Zamil, Z., Zulkifli, N. & Adam, N. Graphene quantum Dots: A comprehensive overview. *Open. Chem.* **21**(1), 20220285. <https://doi.org/10.1515/chem-2022-0285> (2023).
56. Shakourian-Fard, M., Ghenaatian, H. R., Kamath, G. & Taimoory, S. M. Unraveling the effect of nitrogen doping on graphene nanoflakes and the adsorption properties of ionic liquids: A DFT study. *J. Mol. Liq.* **312**, 113400 (2020).
57. Ketabi, N. et al. Tuning the electronic structure of graphene through nitrogen doping: experiment and theory. *RSC Adv.* **6**, 56721–56727 (2016).
58. Sabzevari, M., Cree, D. & Wilson, L. D. Mechanical properties of graphene oxide-based composite layered-materials. *Mater. Chem. Phys.* **234**, 81–89. <https://doi.org/10.1016/J.MATCHEMPHYS.2019.05.091> (2019).
59. Maio, A., Pibiri, I., Morreale, M., Mantia, F. P. & Scaffaro, R. An Overview of Functionalized Graphene Nanomaterials for Advanced Applications. *Nanomaterials* (Basel). ;11(7). (2021).
60. Ioniță, M. et al. Graphene and functionalized graphene: extraordinary prospects for nanobiocomposite materials. *Compos. Part. B: Eng.* **121**, 34–57 (2017).
61. Hermann, J., Distasio, R. A. Jr. & Tkatchenko, A. First-Principles models for Van der Waals interactions in molecules and materials: concepts, theory, and applications. *Chem. Rev.* **117**(6), 4714–4758. <https://doi.org/10.1021/acs.chemrev.6b00446> (2017).
62. Al-Hamdani, Y. S. & Tkatchenko, A. Understanding non-covalent interactions in larger molecular complexes from first principles. *J. Chem. Phys.* **150** (1), 010901 (2019).
63. Hattori, Y., Kaneko, K. & Ohba, T. 5.02 - Adsorption properties. In: (eds Reedijk, J. & Poeppelmeier, K.) *Comprehensive Inorganic Chemistry II* (Second Edition). Amsterdam: Elsevier; 25–44. (2013).
64. Hurd, A. The electrostatic interaction between interfacial colloidal particles. *J. Phys. A Math. Gen.* **18**, L1055 (1999).
65. Cui, L. et al. The interaction energy between solvent molecules and graphene as an effective descriptor for graphene dispersion in solvents. *J. Phys. Chem. C* **125**(9), 5167–5171. <https://doi.org/10.1021/ACS.JPC.0C1013> (2021).
66. Hussain, S. & Maktedar, S. S. Structural, functional and mechanical performance of advanced Graphene-based composite hydrogels. *Results Chem.* **6**, 101029 (2023).
67. Yuan, C. et al. Multistep desolvation as a fundamental principle governing peptide self-assembly through liquid–liquid phase separation. *CCS Chem.* **6**(1), 255–265. <https://doi.org/10.31635/ccschem.023.202302990> (2024).
68. Pratap, B., Gupta, R. K., Bhardwaj, B. & Nag, M. Resin based restorative dental materials: characteristics and future perspectives. *Jpn Dent. Sci. Rev.* **55** (1), 126–138 (2019).
69. Dathan, P., Nair, C., Kumar, A. & Ar, L. Flexural strength is a critical property of dental Materials-An overview. *Acta Sci. Dent. Sciencs.* **7**, 99–103 (2023).
70. he, Y., Zhu, B. & Inoue, Y. Hydrogen bonds in polymer blends. *Progress Polym. Sci. - PROG POLYM. SCI.* **29**, 1021–1051 (2004).
71. Bulusu, G. & Desiraju, G. R. Strong and weak hydrogen bonds in Protein–Ligand recognition. *J. Indian Inst. Sci.* **100**, 31–41. <https://doi.org/10.1007/s41745-019-00141-9> (2020).
72. Grishanov, S. 2 - Structure and properties of textile materials. In: (ed Clark, M.) *Handbook of Textile and Industrial Dyeing*. 1: Woodhead Publishing; 28–63. (2011).
73. Li, X., Wang, X., Zhang, L., Lee, S. & Dai, H. Chemically derived, ultrasmooth graphene nanoribbon semiconductors. *Science* **319** (5867), 1229–1232 (2008).
74. Chen, D., Tang, L. & Li, J. Graphene-based materials in electrochemistry. *Chem. Soc. Rev.* **39**, 3157–3180 (2010).
75. Stankovich, S. et al. Graphene-based composite materials. *Nature* **442** (7100), 282–286 (2006).
76. Zhang, Y., Li, H., Wu, Q. Y. & Gu, L. Non-covalent functionalization of graphene sheets by pyrene-endcapped tetraphenylethene: enhanced aggregation-induced emission effect and application in explosive detection. *Front. Chem.* **10**, 970033 (2022).
77. Park, S. & Ruoff, R. S. Chemical methods for the production of graphenes. *Nat. Nanotechnol.* **4** (4), 217–224 (2009).
78. Cai, D., Jin, J., Yusoh, K., Rafiq, R. & Song, M. High performance polyurethane/functionalized graphene nanocomposites with improved mechanical and thermal properties. *Compos. Sci. Technol.* **72**, 702–707 (2012).

Acknowledgements

The authors extend their gratitude to King Khalid University, Saudi Arabia, for providing financial support. They also sincerely thank Mr. Doni for his invaluable expertise and assistance in the molecular docking and dynamics study conducted for this research.

Author contributions

Conceptualization: M.A.S and R.S.S; methodology: M.A.S and R.S.S; validation: A.H; formal analysis: A.H and S.A.M; investigation: R.S.S and M.S.K; resources: R.S.S and M.S.K; data curation: A.H and S.A.M; writing—original draft preparation: R.S.S; writing—review and editing: M.A.S; supervision: R.S.S; project administration: R.S.S; finding acquisition: M.S.K. All authors have read and agreed to the published version of the manuscript.

Funding

The authors extend their appreciation to the Deanship of Research and Graduate Studies at King Khalid University for funding this work through Large Research Project under grant number RGP2/475/45.

Declarations

Competing interests

The authors declare no competing interests.

Additional information

Supplementary Information The online version contains supplementary material available at <https://doi.org/10.1038/s41598-025-93653-7>.

Correspondence and requests for materials should be addressed to S.A.M. or A.H.

Reprints and permissions information is available at www.nature.com/reprints.

Publisher's note Springer Nature remains neutral with regard to jurisdictional claims in published maps and institutional affiliations.

Open Access This article is licensed under a Creative Commons Attribution-NonCommercial-NoDerivatives 4.0 International License, which permits any non-commercial use, sharing, distribution and reproduction in any medium or format, as long as you give appropriate credit to the original author(s) and the source, provide a link to the Creative Commons licence, and indicate if you modified the licensed material. You do not have permission under this licence to share adapted material derived from this article or parts of it. The images or other third party material in this article are included in the article's Creative Commons licence, unless indicated otherwise in a credit line to the material. If material is not included in the article's Creative Commons licence and your intended use is not permitted by statutory regulation or exceeds the permitted use, you will need to obtain permission directly from the copyright holder. To view a copy of this licence, visit <http://creativecommons.org/licenses/by-nc-nd/4.0/>.

© The Author(s) 2025